Journal of New Materials for Electrochemical Systems 21, 163-170 (2018)

Synthesis and Electrocatalytic Properties of Ni-substituted Co_3O_4 for Oxygen Evolution in Alkaline Medium

Basant Lal[1,*], Ravindra Nath Singh[2] and Narendra Kumar Singh[†,3]

[1]Department of Chemistry, Institute of Applied Science and Humanities, G.L.A. University, Mathura-281406 (U.P.), India
[2]Department of Chemistry, Faculty of Science, Banaras Hindu University, Varanasi-221005 (U.P.) India
[3]Department of Chemistry, Faculty of Science, University of Lucknow, Lucknow-226007, (U.P.) India

Received: February 03, 2018, Accepted: May 28, 2018, Available online: August 20, 2018

Abstract: *Cobalt based Ni-substituted spinel-type oxides were synthesized by carbonate co-precipitation method using Na_2CO_3 as precipitant and studied their electrocatalytic properties towards oxygen evolution reaction (OER) in alkaline medium. Materials were synthesized by using nitrates of nickel and cobalt. For electrochemical studies, oxide powder was transformed in the form of oxide film electrode on nickel substrate. Techniques used were cyclic voltammetry, electrochemical impedance spectroscopy (EIS) and anodic Tafel polarization. Results obtained show that the Ni-substitution in Co_3O_4 matrix increase the oxide roughness factor considerably but did not significantly contribute in electrocatalytic properties for oxygen evolution reaction (OER). Tafel slope and order of reacton with respect to [OH^-] concentration at low overpotential were found to be ~2.303RT/nF and ~1, respectively. The effect of temperature on the electrochemical behaviopur has also been investigated for oxide electrode. Thermodynamic parameters such as, standard electrochemical enthalpy of activation* ($\Delta H_{el}^{0\#}$), *standard enthalpy of activation* ($\Delta H^{0\#}$) *and standard entropy of activation* ($\Delta S^{0\#}$) *were estimated by recording the Tafel polarization curves at different temperatures. X-ray diffraction (XRD), infrared (IR) spectroscopy and scanning electron microscope (SEM) techniques have been used to characterize the materials physicochemically.*

Keywords: Oxygen evolution reaction, Spinel type oxide, Electrocatalysis, Tafel slope, Roughness factor

1. INTRODUCTION

Transition metal mixed oxides of spinel (e.g. Co_3O_4, $CuCo_2O_4$, $NiCo_2O_4$, etc.) and perovskite ($LaCoO_3$, $LaMnO_3$, etc.) families are considered as promising electrode material for the application in electrochemical devices such as water electrolysis cells, fuel cells and metal air batteries [1-8]. Ni-substituted oxide materials were found to be useful in many electrode reactions from O_2 [9] and Cl_2 [10] evolution to O_2 reduction [11] and also in application to metal ion batteries [12,13]. $NiCo_2O_4$ is generally regarded as mixed valent oxide that adopts a spinel structure in which nickel occupies the octahedral site and cobalt is distributed over both octahedral and tetrahedral sites. But, cobalt electrode of these materials obtained by conventional methods usually have low electrochemically active (or real) surface area and hence the electrocatalytic activity. It is, therefore; desire to improve their specific surface area to the reasonable extent.

The efficiency of these oxide materials can be enhanced by developing suitable low temperature preparative methods based on the knowledge of solution chemistry. The textural characteristic and hence the electrochemical interfacial properties of the oxide electrode can also be changed by the partial replacement of constituent metal ion by suitable transition metal ions. Chi et al. [14] synthesized Ni-Co spinel oxide by using different methods and studied the effect on the physicochemical and electrochemical properties. The lattice parameters, crystallite size (S) and surface composition of the material were investigated by De Faria et al. [15]. Recently, B. Cui et al. [16] synthesized core-ring structured $NiCo_2O_4$ nanoplatelets by hydroxide co-precipitation decomposition method and characterized their electrocatalytic properties for the OER. In general, it is observed that both electronic and geometrical factors influence the electrocatalytic properties of the material. The former are governed by the

To whom correspondence should be addressed:
*Email: basant.lal@gla.ac.in
†Email: nksbhu@yahoo.com; Tel.: +91-9451949105

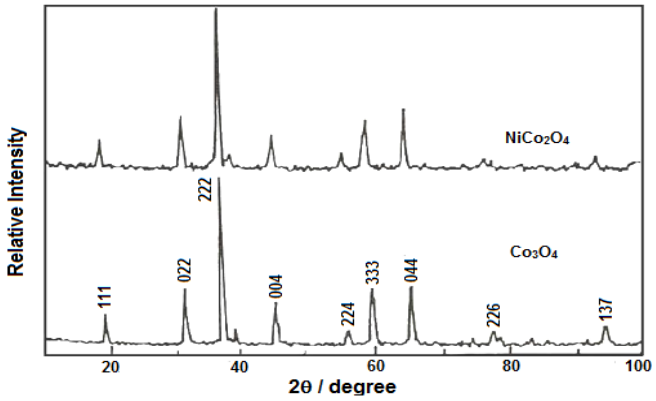

Figure 1. X-ray diffraction of oxide powder sintered at 350 °C for 4 h.

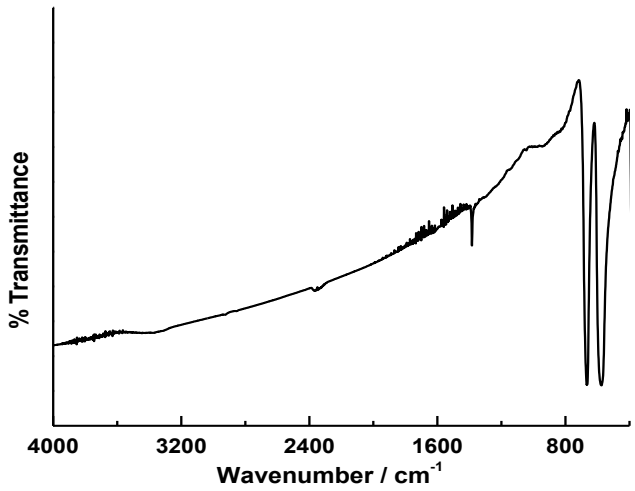

Figure 2. Infrared Spectra (IR) of $NiCo_2O_4$ sintered at 350 °C for 4 h.

electronic structure and the nature of the active sites such as Co^{3+} in $NiCo_2O_4$ [9,17,18], while the latter by the surface concentration of the active sites as well as the extent of actual surface area [15]. In the present investigation, pure and Ni-substituted spinel oxides were synthesized by low temperature carbonate co-precipitation method and studied their physicochemical as well as electrochemical properties with regards to oxygen evolution in alkaline medium. Results, so obtained, are described here.

2. EXPERIMENTAL

Pure and Ni-substituted cobaltites were prepared by carbonate co-precipitation method [19]. In each prerpareation, chemicals and reagents used were of analytical grade and purified. In order to get the desired oxide, aqueous solution of metal nitrates, $Ni(NO_3)_2$, and $Co(NO_3)_2.2H_2O$ (Merck) were taken in stoichiometric ratio and saturated solution of Na_2CO_3 was added to this in a drop wise manner with constant stirring at 60°C, so as to precipitate metal ions as metal carbonate, completely. The precipitate was filtered and washed thoroughly with double distilled water, dried at 120 °C for 12 h and decomposed at 350 °C for 4 h in air to obtained desired oxide. The materials were characterized by recording infrared (IR) spectra (JASCO FT/IR-5300) and XRD powder patterns (Guiner-Wolf Chamber with the Co-K_α-radiation, λ = 0.178889 nm). The morphological information of the oxide powder was obtained by a scanning electron microscope (SEM) using JEOL (JSM 6490). For electrochemical investigation, the oxide film was obtained by painting the slurry of oxide powder with glycerol (2 drops/100 mg of oxide) onto one side of pretreated nickel support (geometrical surface area: 1.5 cm×1 cm, Aldrich 99.9% purity) and on subsequent sintering at 340 °C for 2 h. At temperature below 340 °C, the catalytic film obtained was not reasonably adherent. The procedure adopted for the pretreatment of nickel support and electrical contact is similar to those reported in literature [20, 21].

The electrochemical cell used in this experiment consists of electrolyte, counter electrode (Pt-foil with area 12.3 cm^2, Aldrich 99.9% purity) and reference electrode (Hg/HgO/1M KOH). Instruments used for electrochemical characterizations as well as methodology followed in cyclic voltammetry, electrochemical impedance and Tafel polarization studies were almost similar to those reported in literature [20, 21]. In each experiment, reference electrode is separated from test solution by using luggin capillary containing an aqueous agar-agar (KCl) salt bridge. All the potential values reported in the text correesponds to the reversible potential for the reference electrode Hg/HgO/1M KOH (98 mV vs NHE) only. The instrument used in the investigation was the electrochemical impedance system (EG & G, PARC, USA) comprising with lock-in-amplifier (model 5210), and potentio-galvanostat (model 273A).

3. RESULTS AND DISCUSSION

3.1. XRD, IR and SEM Studies

Formation of spinel phase of Co_3O_4 and its Ni-substituted derivatives was confirmed by XRD powder patterns and IR spectroscopy. Powder X-ray diffraction (XRD) of two representative oxides viz. Co_3O_4 and $NiCo_2O_4$ were recorded between 2θ = 0 and 2θ = 100 and the spectra, so obtained, are shown in Fig. 1. Figure shows that the carbonate method produces almost pure and crystalline nano-sized spinel product and followed cubic crystal geometry (a = b = c and $\alpha = \beta = \gamma = 90°$). The crystallographic density (d) was estimated using the relation, d = 8 M/V, where M and V are corresponding molecular mass and volume of the material assuming 8 molecules of oxide in a unit cell. The cubic cell parameters `a` were computed and found to be ~8.07Å and ~8.13Å for Co_3O_4 and $NiCo_2O_4$, respectively. These values are very close to their respective literature values, 8.08Å (JCPDS ASTM 9-418) and 8.128Å (JCPDS ASTM 20-78).

It is observed that Ni-substitution in Co_3O_4 matrix increased the a-value. similar increase in a-value has also been reported by other worker [9, 22-25] wherein oxides were obtained by other methods. The crystallite size (S) of the oxide was estimated by using Schrrer's formula, $S = 0.9\lambda/\beta \cos\theta$, where, λ is the wavelength of radiation used, β is full width at half maximum of the most intense peak in radian and θ is corresponding angle in degree. The average crystal dimensions were 33.5 nm and 28.4 nm for Co_3O_4 and $NiCo_2O_4$, respectively. The results show that carbonate co-precipitation produces nano sized spinel oxides with comparatively

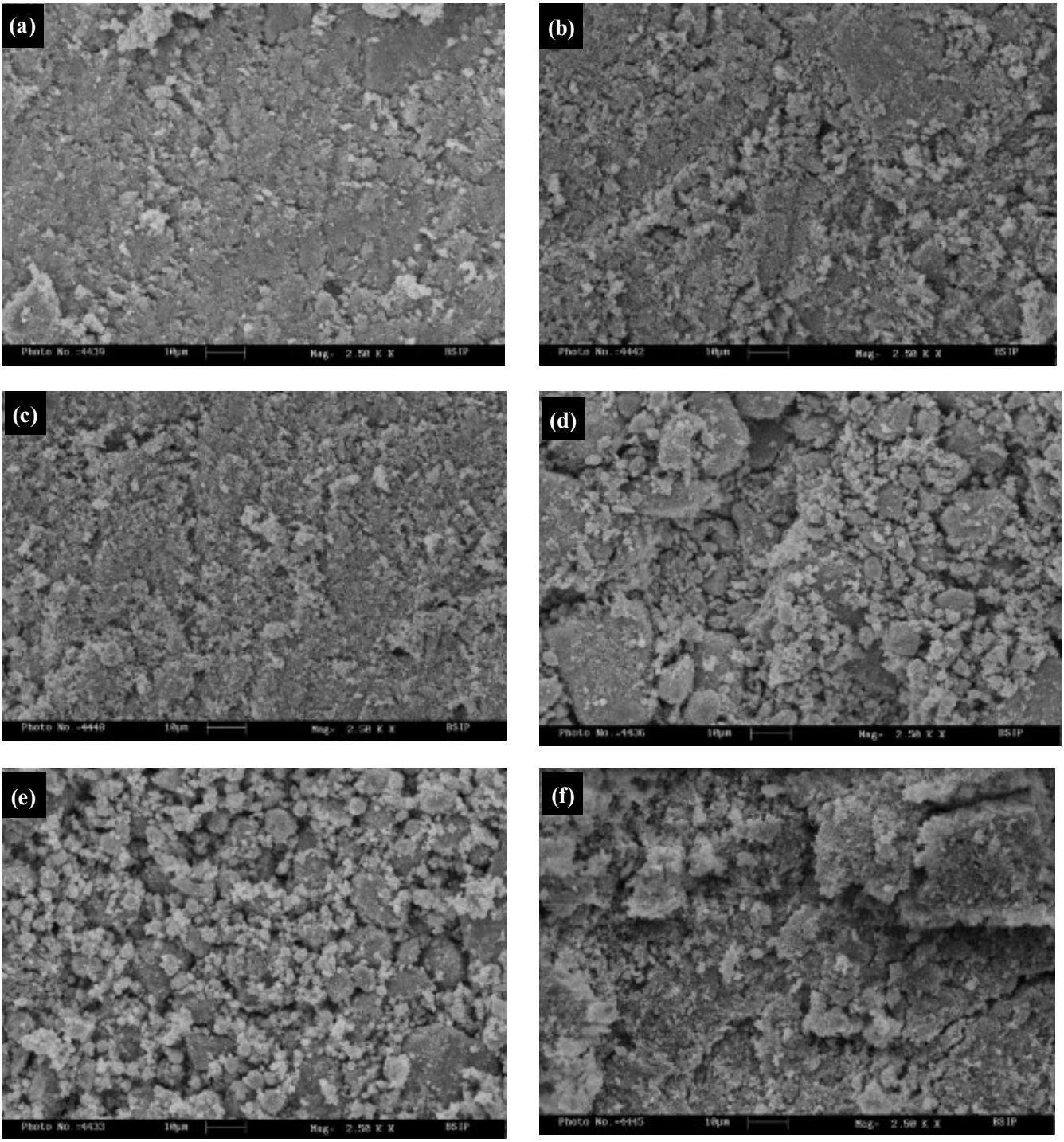

Figure 3. SE-micrograph of the oxode powder sintered at 350 °C for 4 h; a: Co_3O_4, b: $Ni_{0.25}Co_{2.75}O_4$, c: $Ni_{0.5}Co_{2.5}O_4$, d: $NiCo_2O_4$, e: $Ni_{1.2}Co_{1.8}O_4$, f: $Ni_{1.5}Co_{1.5}O_4$

smaller size than those obtained by oxalic acid precipitation method [26]. However, the observed values are larger than those prepared by ethanol evaporation method [27].

Fig. 2 represents the IR-spectra of 1.0 mol Ni-substituted oxide recorded between 4000 – 400 cm^{-1}. The observed two strong peaks at 662 and 565 cm^{-1} corresponds to the pure phase of spinel cobalttite and are ascribed to stretching and bending modes of vibrations of Co^{3+}/ or Ni^{3+} in octahedral site [28].

SE-micrographs of each oxide powder obtained at the magnification × 2500 are shown in the Fig. 3 (a-f). Morphology of each ox-

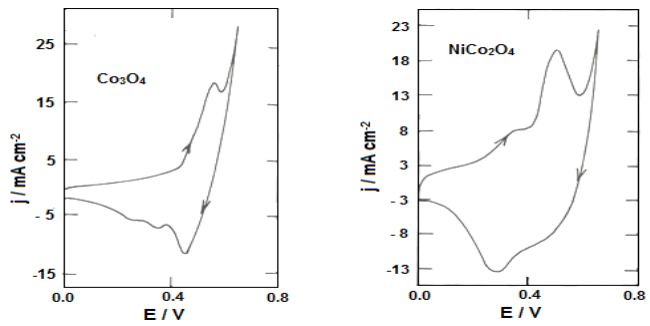

Figure 4. Cyclic voltammogram of the oxide film electrode on Ni in 1M KOH at 25°C (scan rate = 20 mV sec^{-1}).

ide powder was observed to be similar. However, aggregates of large particle have been found with $NiCo_2O_4$, $Ni_{1.2}Co_{1.8}O_4$ and $Ni_{1.5}Co_{1.5}O_4$. Other oxide materials viz. Co_3O_4, $Ni_{0.25}Co_{2.75}O_4$ and $Ni_{0.5}Co_{2.5}O_4$ showed compact texture with smaller particle size.

3.2. Cyclic voltammetry (CV)

In order to investigate the behavior of the oxide surface with regard to oxidation reduction reaction, cyclic voltammogram of pure and Ni-substituted oxides was recorded in 1M KOH over the potential range of 0.0 to 650 mV at the scan rate of 20 mV sec^{-1} at 25 °C. Cyclic voltammetric curves of Co_3O_4 and $NiCo_2O_4$ are given in Fig. 4.

Cyclic voltamogram of Co_3O_4 showed a pair of redox peaks, an anodic and a cathodic, prior to the onset of oxygen evulution reatction. However, in the case of Ni-substituted oxide electrodes, two pairs of redox peaks have been observed. These two different kinds of surface redox processes have Eº values 490±30 and 321±30mV.

Table 1 shows that Eº-value for Co_3O_4 and Ni-substituted cobaltites are 509 mV and 490±30mV corresponding to the redox reaction Co(IV) + e^- ↔ Co(III) [1,29,30]. However, Ni-substituted cobaltites also show another couple of peaks with Eº-value 321±30mV, which corresponds to redox reaction Ni(III) + e^- ↔ Ni(II) [30]. With exception of 0.5 mol Ni, substitution of nickel for cobalt in Co_3O_4 matrix marginally reduces the Eº-value and this effect of reduction is being observed maximum in case of 1.0 mol Ni-substituted oxide. The values of peak potentials E_{pa} and E_{pc}, the formal redox potential (E^o= (E_{pa}+E_{pc})/2) were analyzed from the cyclic voltammetric curve and are listed in Table 1.

3.3. Impedance spectroscopy/Roughness factor (R_F)

The electrochemically active area of the oxide electrode is determined in terms of roughness factor. For the purpose, impedance spectra were recorded at three different potentials 0, 50 and 100 mV in 1 M KOH at 25°C in the frequency range from 0.1 to 10^5 Hz. The DC potentials chosen were in the region wherein the contribution of faradic processes was practically negligible as it is quite evident from cyclic voltammogram shown in Fig. 4. The capacitance double layer (C_{dl}) of the catalyst/1M KOH interface was determined by analyzing impedance data using series LRQC equivalent circuit model [31], where L, R, Q and C are the inductance (henri), resistance (ohm), constant phase element (FS^{n-1}) and capacitance (farad), respectively. The series model is fairly reproduced the feature of experimental curves. Some representative impedance spectra in both Nyquist and Bode model at 50 mV are shown in Fig. 5 (a & b). Relative values of oxide roughness factor was determined from the C_{dl} value of the oxide/solution interface by assuming 60μF cm^{-2} as the C_{dl} for smooth oxide surface [1,9,32]. The value of C_{dl} and other circuit parameters determined at three DC potentials were approximately the same and their average values are given in Table 2. The introduction of Ni in Co_3O_4 matrix increases the oxide roughness factor and it is found to be higher in the case of lower Ni-substitution (i.e. in 0.25 and 0.5 mol). It is noteworthy that the roughness factor of oxides produced by this method is, in general, higher than those reported for the similar oxide film electrodes prepared by other methods. For example, the Co_3O_4 film electrode on Ni, Ti, and Cd/glass prepared by spraying [20], on Ni prepared by sequential solution coating [9] and hydroxide co-precipitation method [24] were ~530, ~9, and ~63, respectively. While, the present method produced the oxide roughness ~1030 for the same oxide on Ni. Similarly, $NiCo_2O_4$ obtained by this method exhibited many times higher roughness than the same oxide obtained by spray pyrolysis method on Ni [20]. However, this value was similar to that the same oxide film obtained by the hydroxide co-precipitation method [24] (R_F = 1460). It is worth mentioning that the R_F values quoted in the literature were determined by cyclic voltammetry.

3.4. Electrocatalytic activity

The electrocatalytic activity of pure and Ni-substituted Co_3O_4 have been examined with respect to the electrolytic oxygen evolution reaction (OER) in 1M KOH at 25°C. For the purpose, the anodic polarization curves were recorded for each oxide catalyst in 1M KOH at the scan rate of 0.2 mV sec^{-1}. The polarizaiton curve,

Table 1. Values of cyclic voltammetric parameters for OER on pure and Ni-substituted cobaltites electrode in 1M KOH at 25°C.

Electrode	E_{pa} /mV	E_{pc} /mV	ΔE_p /mV	ΔE^0_p /mV	E'_{pa} /mV	E'_{pc} /mV	$\Delta E'_p$ /mV	$\Delta E^{0'}_p$ /mV
Co_3O_4	560	458	102	509	-	-	-	-
$Ni_{0.25}Co_{2.75}O_4$	557	435	94	496	368	333	35	351
$Ni_{0.5}Co_{2.5}O_4$	586	454	132	520	382	254	128	318
$NiCo_2O_4$	512	408	104	460	350	303	47	327
$Ni_{1.2}Co_{1.8}O_4$	542	436	106	489	306	282	24	294
$Ni_{1.5}Co_{1.5}O_4$	539	432	107	486	354	276	80	315

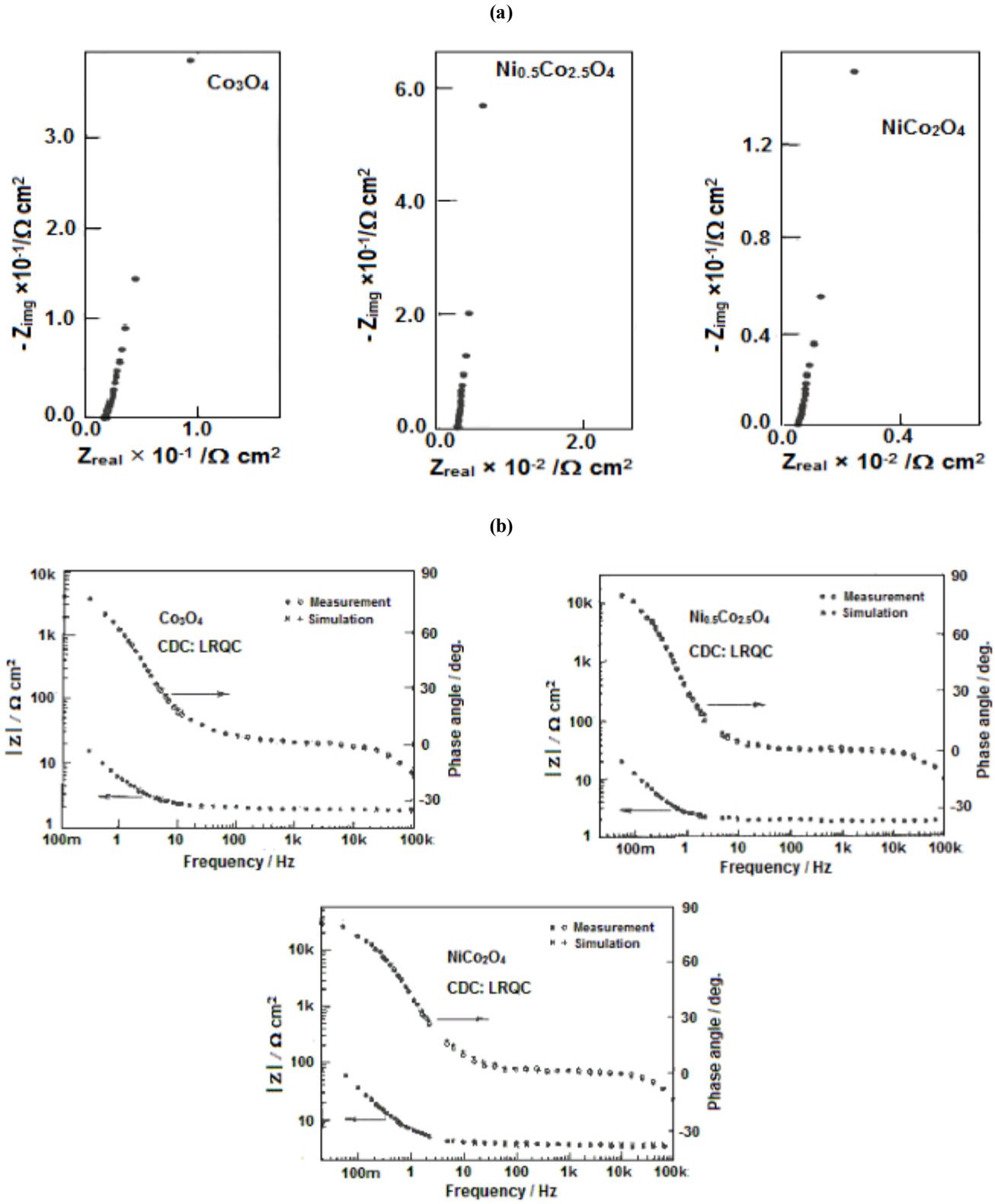

Figure 5. (a): Complex impedance (Nyquist) plots for Co_3O_4, $Ni_{0.5}Co_{2.5}O_4$ and $NiCo_2O_4$ electrodes in 1M KOH at E = 50 mV (25 °C). (b): Bode plots for Co_3O_4, $Ni_{0.5}Co_{2.5}O_4$ and $NiCo_2O_4$ electrodes in 1M KOH at E = 50 mV (25 °C).

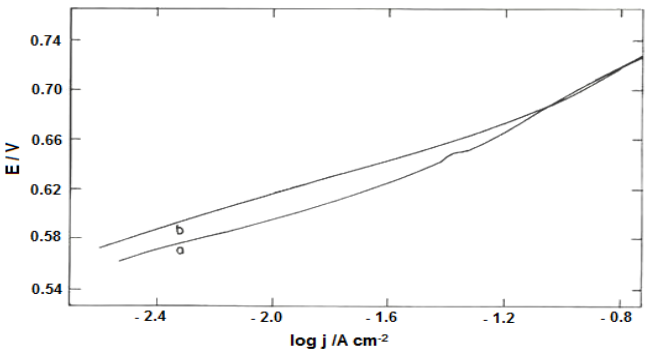

Figure 6. iR-free Tafel plots on the cobaltite film electrode on Ni in 1M KOH at 25 °C (scan rate 0.2 mV sec^{-1}); (a) Co_3O_4 and (b) $NiCo_2O_4$

so recorded, was almost similar with each catalyst and representative polarization curves for Co_3O_4 and $NiCo_2O_4$ are shown in Fig. 6. Values of Tafel slope corresponding to each polarization curve were estimated from the polarization curve and found to be ranged between 63-74 mV $decade^{-1}$ and 98-134 mV $decade^{-1}$ at lower and higher potential region, respectively. To compare the electrocatalytic activity of catalysts, the apparent current density (j_a) and true current density (j_t) determined at two potentials 650 and 700 mV from polarization curves are given in Table 3. It is observed that j_a-value at both potentials did not follow a definite pattern with Ni-substitution in cobaltite matrix. However, j_t-value at both potentials reduces considerably with Ni-substitution in cobaltite matrix and maximum reduction observed with $NiCo_2O_4$.

To determine the order of reaction (p) with respect to [OH^-] for OER, the anodic Tafel polarization curves on Co_3O_4 and $NiCo_2O_4$ were recorded at varying KOH concentrations keeping the ionic strength (μ) of the medium and temperature constant. The ionic strength of the medium was maintained constant by using KNO_3 as an inert electrolyte. The order of OER was estimated from the slope of linear plot log j vs log [OH^-] (Fig. 7) and found to be approximately unity (1.0 & 1.2). Values of Tafel slopes and order for OER on electrocatalysts suggest that the electroformation of oxygen on the oxide catalysts follows almost similar mechanistic paths, regardless of the Ni-substitution in Co_3O_4 matrix.

The influence of temperature on the OER has also been investigated on some oxide catalysts (viz., Co_3O_4, $Ni_{0.25}Co_{2.75}O_4$ and $NiCo_2O_4$) at different temperatures 30, 40, 50, 60 and 70 °C. The standard apparent electrochemical activation energy ($\Delta H_{el}^{\#0}$) was determined by constructing the Arrhenius plot (log j vs 1/T) at constant applied potential (640 mV) in first Tafel region and shown in Fig. 8. The electrochemical activation energy ($\Delta H_{el}^{\#0} = slope \times 2.303R$) was calaulated by measuring the slope of the plot. The charge transfer coefficient (α) and standard activation energy ($\Delta H^{\#0}$) were estimated from b values at different temperatures and by using the relation $\Delta H^{\#0} = \Delta H_{el}^{\#0} + \alpha FE$, respectively. The average values of electrochemical activation energy ($\Delta H_{el}^{\#0}$), charge transfer coefficient (α) and standard activation energy ($\Delta H^{\#0}$) are given in Table 4.

The standard entropy of reaction ($\Delta S^{\#0}$) has also been calculated by using the following relation [33].

$$\Delta S^{\#0} = 2.303R \left[\frac{\Delta H_{el}^{\#0}}{2.303RT} + \log j - \log nF\omega C_{OH^-} \right]$$

where ω = kT/h and n = 2 and other terms involved in the

Table 2. Values of equivalent circuit parameter for OER on pure and Ni-substituted cobaltites in 1M KOH at 25°C.

Electrode	Loading (mg cm^{-2})	L × 10^6 (heneri)	R (ohm)	Q × 10 (FS^{n-1})	n	C × 10^3 (mF)	R_F	R_F (mg^{-1})
Co_3O_4	5.4±1.0	1.04±0.21	2.4±0.5	0.87±0.11	0.6±0.1	61.8±1.8	1030±30	~191
$Ni_{0.25}Co_{2.75}O_4$	4.8±0.1	0.89±0.01	2.3±0.1	3.14±0.16	0.7±0.1	122.6±4.1	2042±68	~425
$Ni_{0.5}Co_{2.5}O_4$	5.5±0.1	0.89±0.04	2.0±0.1	6.92±0.98	0.5±0.1	135.3±6.1	2254±101	~410
$NiCo_2O_4$	5.5±0.1	0.73±0.03	2.7±0.2	4.41±.77	0.4±0.1	97.9±1.2	1631±21	~297
$Ni_{1.2}Co_{1.8}O_4$	5.1±0.4	0.95±0.11	1.7±0.1	2.41±0.13	0.3±0.1	112.0±1.8	1867±30	~366
$Ni_{1.5}Co_{1.5}O_4$	5.5±1.0	0.61±0.11	1.9±0.2	5.96±0.14	0.2±0.1	89.6±1.9	1494±33	~272

Table 3. Values of electrode kinetic parameter for OER on pure and Ni-substituted cobaltites 1M KOH at 25°C.

Electrode	Loading (mg cm^{-2})	Tafel slope /mV $dcade^{-1}$		Order (p)	j/mA cm^{-2} at E/mV			
		b_1	b_2		650		700	
					j_a	$j_t \times 10^2$	j_a	$j_t \times 10^2$
Co_3O_4	5.4±0.2	66	134	1.2	9.9±3.2	1.10	230±8.5	22.3
$Ni_{0.25}Co_{2.75}O_4$	4.8±0.1	72	101	-	9.8±0.8	0.48	164±5.6	8.0
$Ni_{0.5}Co_{2.5}O_4$	5.5±0.1	74	114	-	15.4±0.7	0.68	223±0.5	9.9
$NiCo_2O_4$	5.5±0.2	63	101	1.0	4.9±1.0	0.30	112±8.0	6.8
$Ni_{1.2}Co_{1.8}O_4$	5.1±0.4	71	98	-	12.6±3.7	0.67	168±12.5	9.0
$Ni_{1.5}Co_{1.5}O_4$	5.5±0.5	68	104	-	10.4±2.9	0.69	144±0.2	9.6

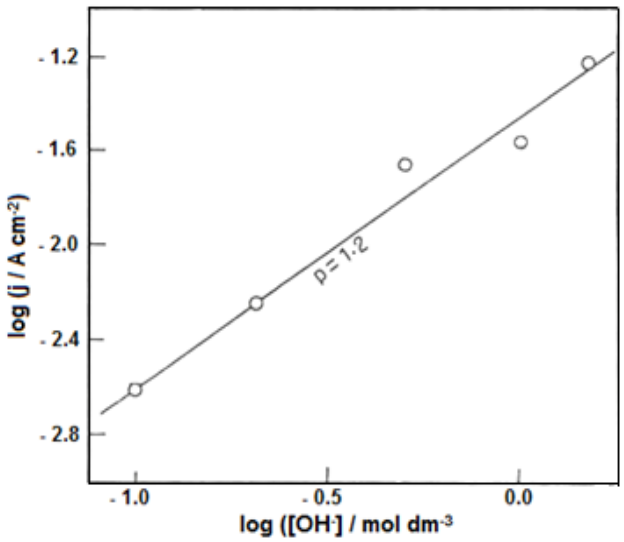

Figure 7. Plot of log j vs log [OH^-] (μ = 1.5) for Co_3O_4 at constant applied potential (E = 0.64 V) across catalyst/ KOH solution interface at 25 °C.

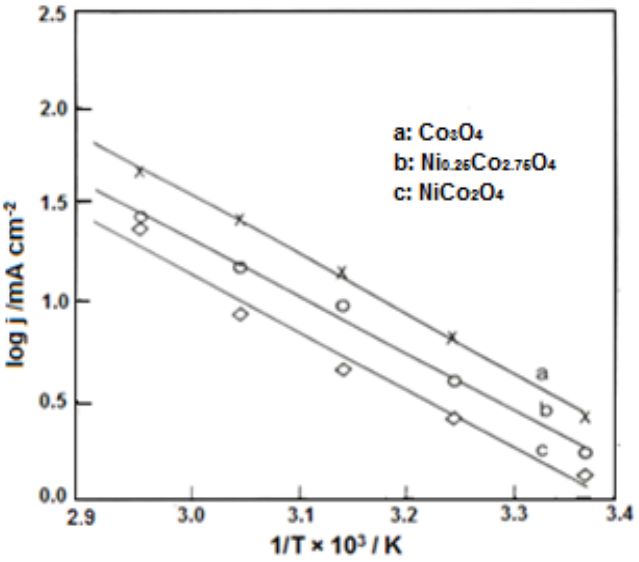

Figure 8. Arrhenius plots at a constant applied potential (E = 0.64V) across the oxide/1M KOH solution interface.

equation have their usual meaning. Table 4 shows that 0.25, 0.5 and 1.0 mol Ni-substitution in Co_3O_4 matrix decrease the $\Delta H_{el}^{\#0}$ and $\Delta H^{\#0}$ -values for OER, the magnitude of reduction being the greatest in 0.5 mol Ni in both the cases. Value of Tafel slope (b_1) increased slightly with rise in temperature from 30 to 70^0C. The increase in b_1 values were 50 to 59, 72 to 78 and 64 to 72 mV $decade^{-1}$ for Co_3O_4, $Ni_{0.25}Co_{2.75}O_4$ and $NiCo_2O_4$, respectively. The increase in the b_1 value with rise in temperature is not usual but it is demanded as per its definition, $b = \frac{2.303RT}{\alpha F}$. The charge transfer coefficient (α) value was observed to be almost constant with each electrocatalyst. The values of the standard entropy of activation ($\Delta S^{\#0}$) for OER on Co_3O_4 and its Ni-substituted derivatives were found to be highly negative and not much different also, regardless of nature of catalysts. The highly negative value of $\Delta S^{\#0}$ indicate that the reaction of oxygen evolution is followed through formation of similar adsorption intermediate.

4. CONCLUSION

The result showed that co-precipitation method produces single phase nano-sized spinel type oxides with enhanced surface area and hence high electrocatalytic activity. The Ni-substitution in Co_3O_4 matrix considerably improves the oxide roughness factor and found to be greatest with the 0.5 mol Ni-substitution. However, the substitution of nickel did not affect the electrocatalytic activity of the material significantly.

5. ACKNOWLEDGEMENTS

Authors owe the debt of gratitude to head of Department of Chemistry, Banaras Hindu University, Varanasi for providing required facilities to carry out this investigation.

REFERENCES

[1] Singh R. N., Koenig J. F., Poillerat G., Chartier P., *J. Electrochem. Soc*., 137, 1408 (1990).

[2] Rasiyah P., Tseung A. C. C., *J. Electrochem. Soc*., 130, 2384 (1993).

[3] Daghetti A., Lodi G., Trasatti S., *Mater. Chem. Phys*., 8, 1 (1983).

[4] Baydi M. El., Tiwari S. K., Singh R. N., Rehspringer J. L., Chartier P., Koenig J. F., Poillerat G., Solid State Chem., 116, 157 (1995).

[5] Tiwari S. K., Samuel S., Singh R. N., Poillerat G., Koenig J. F.,

Table 4. Values of thermodynamic parameter for OER on pure and Ni-substituted cobaltites 1M KOH.

Electrode	Charge transfer coefficient (α)	$\Delta H_{el}^{\#0}$ /kJ mol^{-1} at E = 0.58 V	$\Delta H^{\#0}$/ kJ mol^{-1} calculated from b-value	$-\Delta S^{\#0}$ /J $deg^{-1}mol^{-1}$
Co_3O_4	1.13	58.1	120.2	182.4
$Ni_{0.25}Co_{2.75}O_4$	0.86	48.2	97.2	200.8
$Ni_{0.5}Co_{2.5}O_4$	0.76	46.9	88.9	205.0
$NiCo_2O_4$	0.93	54.6	107.4	184.9

Chartier P., Int. J. Hydrogen Energy, 9, 20 (1995).
[6] Boca C., Barbucci A., Delicchi M., Cerisola G., Int. J. Hydrogen Energy, 24, 21 (1999).
[7] Suffredini H. B., Cerne J. L., Crnkovic F. C., Machado S. A. S., Avaca L. A., Int. J. Hydrogen Energy, 25, 415 (2000).
[8] Chi B., Li J. B., Han Y. S., Chem Y. J., Int. J. Hydrogen Energy, 29, 605 (2004).
[9] Marsan B., Fradette N., Beaudoin G., J. Electrochem. Soc., 139, 1889 (1992).
[10]Bogglo R., Carugati A., Lodi G., Trasatti S., J. Appl. Electrochem., 15, 335 (1985).
[11]Singh R. N., Koenig J. F., Poillerat G., Chartier P.,J. Electr oanal. Chem., 314, 241 (1991).
[12]Alcantara R., Jaraba M., Lavela P., Tarado J. L., Chem. Mater., 14, 2847 (2002).
[13]Chardvick A. V., Savin S. L. P., Fiddy S., Alcantara R., Lisbona D. F., Lavela P., Ortiz G. F., Tirado J. L., J. Phys. Chem. C, 111, 4636 (2007).
[14]Chi B., Li J. B., Han Y. S., Dai J. H., Mater. Lett., 58, 1415 (2004).
[15]De Faria L. A., Prestat M., Koenig J. F., Chartier P., Trasatti S., Electrochim. Acta., 44, 1481 (1998).
[16]Cui B., Lin H., Li J. B., Li X., Yang J., Tao J., Adv. Funct. Mater., 18, 1440 (2008).
[17]Svegl F., Orel B., Hutchins M. G., Kalcher K., J. Electrochem. Soc., 143, 1532 (1996).
[18]Estrada W., Fantini M. C. A., de Castro S. C., Polo da Foneea C. N., Gorenstein A., J. Appl. Phys., 74 5835 (1993).
[19]Huili G., Dai L. Z., Lu D. S., Peng S. Y., J. Solid State Chem., 89, 167 (1990).
[20]Singh S. P., Samuel S., Tiwari S. K., Singh R. N., Int. J. Hydrogen Energy, 21(3), 171 (1996).
[21]Singh N. K., Tiwari S. K., Anitha K. L., Singh R. N., J. Chem. Soc. Faraday Trans., 92, 2397 (1996).
[22]Nikolov I., Darkaoui R., Zhecheva E., Stoyanova R., Dimitrov N., Vitano T., J. Electroanal. Chem., 429, 157 (1997).
[23]Singh J. P., Singh R. N., J. New Mat. Electrochem. System, 3, 131 (2000).
[24]Gennero De Chialvo M. R., Chialvo A .C., Electrochim. Acta, 38, 2247 (1993).
[25]Rios E., Nguyen-Cong H., Marco J. F., Gancedo J. P., Chartier P., Gautier J. L., Electrochim. Acta, 45, 4431 (2000).
[26]Chang S. K., Zainal Z., Tan K. B., Yusof N. A., Yusof W. M. D.W., Prabhakaran S. R. S., Sains Malaysiana, 41(4), 465 (2012).
[27]Cabo M., Pellicer E., Rossinyol E., Estrader M., Ortega A. L., Nogues J., Castell O., Surinnach S., Baro M. D., J. Mater. Chem., 20, 7021 (2010).
[28]Nkeng P., Poillerat G., Koenig J. F., Chartier P., Lefez B., Lenglet M., ECASIA, CA-16, 207 (1993); Poillerat G., Journal de Physique, , 4 C1, 107 (1994).
[29]Baggio R., Carugati A., Trasatti S., J. Appl. Electrochem., 17, 828 (1987).
[30]Hamdani M., Koenig J. F., Chartier P., J. Appl. Electrochem., 18, 568 (1988).
[31]Baukamp B. A., Solid State Ionics, 20, 31 (1986).
[32]Levine S., Smith A. L., Discuss Faraday Soc., 52, 290 (1971).
[33]Gileadi E., Electrode Kinetics (VCH Publishers Inc. New York), p. 151 (1993).